Modeling the effect of position-dependent random dopant fluctuations on the process variability of submicron channel MOSFETs through charge-based compact models: a

Modeling the effect of position-dependent random dopant fluctuations on the process variability of submicron channel MOSFETs through charge-based compact models: a Green's function approach

L. Masoero, F. Bonani, F. Cappelluti, G. Ghione

Dipartimento di Elettronica, Politecnico di Torino, Corso Duca degli Abruzzi 24, 10129 Torino, Italy

***Abstract*—This paper presents an analytical approach, based on a compact MOSFET model, to evaluate the statistical properties of current fluctuations induced by the variability of the channel doping profile. The method is founded on a linear perturbation theory, whereby the total current fluctuation results as a spatial superposition integral involving the random dopant fluctuation arising from process variability and, as the kernel, the Green's function that describes the current fluctuation caused by a spatially impulsive doping fluctuation. The paper focuses on the evaluation of the Green's function through a surface-potential based charge-control compact model; the result is shown to be in good agreement with the same Green's function, as evaluated through a 2D numerical drift-diffusion model, also for short-gate devices. This suggests that, with the application of proper heuristic parametrization, the compact model may be able to provide predictive results also for deeply-scaled MOSFET technologies.**

I. Introduction

The analysis and modeling of the effect of random process variations on the electrical device performances (the so-called *variability analysis*) has become of primary importance in the design of MOSFET-based circuits exploiting deeply scaled technologies [1], [2], [3]. Of course various degrees of variability are possible [1], going from the wafer level, where process variations are the major cause of variability, to the device level. Within this work, we shall concentrate to the treatment of device level variations only.

Among the possible causes for device level variation (namely, metal gate work function variations, process variation effects and random dopant fluctuations), a major role in influencing the variability of electrical performances is played by the intrinsic granularity of doping inside the device channel [3]. From the standpoint of modeling, the effect of random, space dependent dopant fluctuations, has been up to now mainly analyzed through physics-based, numerical 2D or 3D simulations. Representative examples of exploited approaches are the drift-diffusion transport model (including, in some cases, quantum corrections based on the density gradient method) [3], [4], [5] or more complete, higher-order carrier transport models [6], that should be more accurate in describing deeply scaled devices. Some analytical models have also been proposed to model the effect of a channel random dopant distribution [2], [7]; however, they are limited to assessing the effect of dopant fluctuations on the threshold voltage through a solution of Poisson's equation in the absence of current flow: a purely electrostatic problem is solved and the effect of carrier transport is not considered.

In this contribution, we propose a general methodology to include the effect of device-level position-dependent random doping fluctuations into charge-based compact MOSFET models. The approach can be of course applied to evaluating the same effect in other FET technologies. The effect of the technological variations of local doping is directly estimated in terms of the drain current fluctuations with respect to the value obtained with nominal doping, rather than from the variations induced in the threshold voltage only. To this aim, a linear perturbation approach is exploited, in agreement with threshold voltage modeling analyses presented in [2], [7], and the cumulative effect of doping fluctuations on the drain current fluctuation is estimated through a Green's function approach.

The present paper focuses on the evaluation of the Green's function within the framework of a compact modeling approach. Preliminary results are presented, showing that the Green's function can be accurately estimated through surface potential-based compact models also for comparatively short channel MOSFETs (see Sec. IV). To keep the model complexity under control, we consider for the moment a uniformly doped device structure with constant mobility; the inclusion of retrograde profiles and velocity saturation will be presented elsewhere, and will be based on the modeling strategy implemented into the PSP compact model [8].

The paper is structured as follows. Sec. II introduces the variability model based on the linear perturbation approach and provides some general insight into the solution method. Sec. III presents a detailed analysis of the model framework and of the Green's function derivation within the framework of a surface potential compact MOSFET model. Sec. IV is devoted to a validation of the analytical, compact-model based Green's function approach through comparison with 2D drift-diffusion simulations; it is shown that the Green's function as it is derived from the present approach is in good agreement

with the 2D drift-diffusion result also for comparatively short-channel devices, which suggests that, with the help of proper heuristic corrections, the model can be predictive also within the framework of deeply-scaled technologies. Finally, Sec. V reports some conclusions and future developments.

II. The Linear Perturbation-Based Variability Model

Due to the complexity of the interactions (electrostatic, transport-related) included in a device model, the functional relationship between the dopant distribution and the DC current resulting from the application of a given bias condition is generally expected to be nonlinear. However, if we focus on the DC current *deviations* with respect to a nominal value, induced by a dopant variation vs. a nominal or ideal doping profile, a linear relationship is granted to hold in the limit of small variations. Indeed, literature results concerning the analysis of threshold voltage variability vs. dopant fluctuations suggest that a linear perturbation theory may be accurate enough in practical situations, besides being at any rate a first modeling step, see [2], [7].

In the present approach, we assume therefore that the doping variations linearly perturb the nominal device current. This will allow us to exploit a Green's function approach plus spatial superposition akin to the general methodology used for device noise analysis [9], [10] and for linear sensitivity analyis [11], [12], [13]. According to the afore-mentioned technique, the drain current variation δI_{D} resulting from a doping variation is therefore obtained as the output of a two-step approach:

- the deterministic Green's function relating the doping fluctuations to the drain current variations is calculated by linearizing the perturbed compact model equations, using as a source term an impulsive doping variation $\delta N_{\mathrm{A}}(\mathbf{r}) = C\delta(\mathbf{r}-\mathbf{r}_0)$ (where $\mathbf{r}_0$ is the injection point into the channel);
- The current variation δI_{D} is finally calculated as a spatial superposition integral whose kernel is the Green's function and whose input data is a space-dependent random process describing the doping fluctuations along the channel.

This linear perturbation approach was already proposed in [5] within the framework of the drift-diffusion model, and is currently implemented into the Sentaurus Device TCAD suite by Synopsys [14]. The scheme of the simulation technique is reported in Fig. 1, where the box represents the numerical solution of the physical model.

The definition of the nominal device structure and bias allows to determine the corresponding current value I_{D}. Once the nominal solution is known, the doping fluctuation δN_{A} is added to the model and, under the assumption of linear perturbation, the induced current fluctuation is given by the superposition integral

$$\delta I_{\mathrm{D}} = \int_{\Omega} G_{3\mathrm{D}}(\mathbf{r})\delta N_{\mathrm{A}}(\mathbf{r})\ \mathrm{d}\mathbf{r} \tag{1}$$

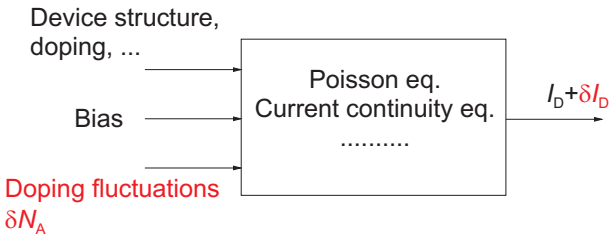

Fig. 1. Schematic representation of the linear perturbation-based simulation technique.

where Ω represents the device domain. Clearly, (1) yields the definition of the Green's function as the result of the application of an impulsive doping fluctuation:

$$G_{3\mathrm{D}}(\mathbf{r}_0) = \frac{1}{C}\,\delta I_{\mathrm{D}}|_{\delta N_{\mathrm{A}}=C\delta(\mathbf{r}-\mathbf{r}_0)}\,. \tag{2}$$

If the statistics of the doping fluctuations is simply described e.g. as a zero-average Gaussian random variable, linear system theory immediately yields a straightforward relationship between the doping fluctuation variance and the variance of the resulting current fluctuations. In fact, from (1)

$$\sigma_{\delta I_{\mathrm{D}}} = \left\langle \delta I_{\mathrm{D}}^2 \right\rangle = \int_{\Omega}\int_{\Omega} G_{3\mathrm{D}}(\mathbf{r}_1)\sigma_{\delta N_{\mathrm{A}}}(\mathbf{r}_1,\mathbf{r}_2)G_{3\mathrm{D}}(\mathbf{r}_2)\ \mathrm{d}\mathbf{r}_1\mathrm{d}\mathbf{r}_2 \tag{3}$$

where $\langle\cdot\rangle$ denotes the statistical average and $\sigma_{\delta N_{\mathrm{A}}}(\mathbf{r}_1,\mathbf{r}_2) = \langle \delta N_{\mathrm{A}}(\mathbf{r}_1)\delta N_{\mathrm{A}}(\mathbf{r}_2)\rangle$ is the spatial correlation function associated to the doping fluctuations.

The expression in (3) can be significantly simplified if we can assume that individual dopants are randomly and independently placed according to a Poisson statistical distribution [5], since in this case spatial uncorrelation results

$$\sigma_{\delta N_{\mathrm{A}}}(\mathbf{r}_1,\mathbf{r}_2) = N_{\mathrm{A}}(\mathbf{r}_1)\delta(\mathbf{r}_1-\mathbf{r}_2) \tag{4}$$

yielding

$$\sigma_{\delta I_{\mathrm{D}}} = \int_{\Omega} G_{3\mathrm{D}}^2(\mathbf{r}_1)N_{\mathrm{A}}(\mathbf{r}_1)\ \mathrm{d}\mathbf{r}_1. \tag{5}$$

Notice that (3) and (5) are derived for a 3D model. However, as discussed in [5], $G_{3\mathrm{D}}(\mathbf{r})$ can be derived starting from 2D simulations of the cross section provided that the device average doping is homogeneous in the width direction z. This ultimately allows a compact model to be exploited to evaluate the effect of 3D doping fluctuations.

Simplifications are of course required to allow for an analytical evaluation of the Green's function, as necessary for the derivation of a compact model. In fact, the physical model has to be consistently simplified to yield the expression forming the basis of the compact model, e.g. decoupling the field components according to the gradual channel approximation.

Notice, finally, that a major (and possibly critical) role in this methodology is played by the definition of the correct shape of the doping fluctuation, which, besides from (4), can also be obtained numerically, e.g. starting from more fundamental, physics-based statistical process simulations. In the following section, the general procedure outlined so far

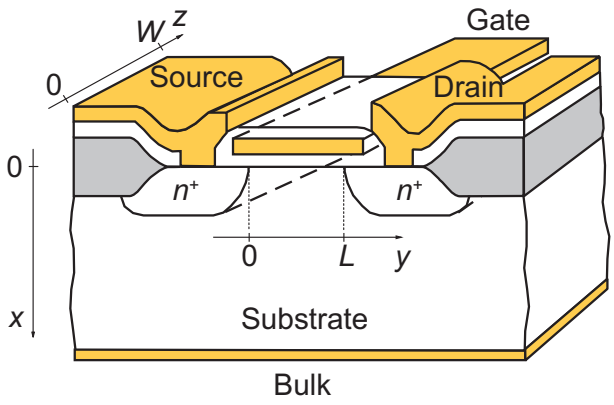

Fig. 2. Structure of the MOSFET considered in the model derivation.

will be specifically applied to a potential-based charge-control compact MOSFET model.

III. The Analytical Green's Function Derivation

For the sake of definiteness, we consider the simplified nMOS device structure in Fig. 2. According to [15], in inversion operation, and within the charge sheet approximation, the total charge (per unit area) present on the gate Q_t and the depletion charge Q_d are related to the surface potential $\psi_\mathrm{s}(y)$ (referred to the bulk) controlling the depletion layer width by:

$$Q_\mathrm{t}(y) = \sqrt{2q\epsilon_\mathrm{S}N_\mathrm{A}}\sqrt{\psi_\mathrm{s}(y) + \frac{n_\mathrm{i}^2}{N_\mathrm{A}^2}V_T\mathrm{e}^{(\psi_\mathrm{s}(y)-\xi(y))/V_T}} \tag{6}$$

$$Q_\mathrm{d}(y) = -\sqrt{q\epsilon_\mathrm{S}N_\mathrm{A}\psi_\mathrm{s}(y)}, \tag{7}$$

respectively. In the previous equations, q is the electron charge (absolute value), ϵ_S the Si permittivity, N_A the substrate doping, n_i the Si intrinsic concentration, V_T the thermal voltage, $\xi(y)$ the quasi-Fermi level splitting in the Si (ultimately related to the source and drain potentials). The surface potential is given by the equation [15], [16]:

$$\begin{aligned} V_\mathrm{GB} - V_\mathrm{FB} - \psi_\mathrm{s}(y) &= \frac{Q_\mathrm{t}(y)}{C_\mathrm{ox}} \\ &= \gamma\sqrt{\psi_\mathrm{s}(y) + \frac{n_\mathrm{i}^2}{N_\mathrm{A}^2}V_T\mathrm{e}^{(\psi_\mathrm{s}(y)-\xi(y))/V_T}} \end{aligned} \tag{8}$$

where V_GB is the gate-bulk voltage, V_FB the MOS flat band voltage, $\gamma = \sqrt{2q\epsilon_\mathrm{S}N_\mathrm{A}}/C_\mathrm{ox}$ the body effect coefficient and C_ox the oxide capacitance per unit gate area. Charge conservation yields the inversion charge $Q_n(y)$ as $Q_n(y) = -Q_\mathrm{t}(y) - Q_\mathrm{d}(y)$. Finally, the drain current is related to the inversion charge and the surface potential by:

$$I_\mathrm{D} = -W\mu_n\left[Q_n\frac{\mathrm{d}\psi_\mathrm{s}}{\mathrm{d}y} - V_T\frac{\mathrm{d}Q_n}{\mathrm{d}y}\right]. \tag{9}$$

A space-dependent doping fluctuation $\delta N_\mathrm{A}(y)$ induces charge and surface potential variations $\delta Q(y)$ and $\delta\psi_\mathrm{s}(y)$, respectively. Linearizing (6) and (7) we find:

$$\delta Q_\mathrm{t}(y) = \alpha\delta N_\mathrm{A} + \theta\delta\psi_\mathrm{s} \tag{10}$$

$$\delta Q_\mathrm{d}(y) = -\frac{\sqrt{2q\epsilon_\mathrm{S}}}{2}\frac{N_\mathrm{A}\delta\psi_\mathrm{s} + \psi_\mathrm{s}\delta N_\mathrm{A}}{\sqrt{N_\mathrm{A}\psi_\mathrm{s}}}, \tag{11}$$

where

$$\alpha(y) = \frac{\sqrt{2q\epsilon_\mathrm{S}}}{2\sqrt{N_\mathrm{A}}}\frac{\psi_\mathrm{s}(y) - V_T\frac{n_\mathrm{i}^2}{N_\mathrm{A}^2}\mathrm{e}^{(\psi_\mathrm{s}(y)-\xi(y))/V_T}}{\sqrt{\psi_\mathrm{s}(y) + V_T\frac{n_\mathrm{i}^2}{N_\mathrm{A}^2}\mathrm{e}^{(\psi_\mathrm{s}(y)-\xi(y))/V_T}}} \tag{12}$$

$$\theta(y) = \frac{\sqrt{2q\epsilon_\mathrm{S}N_\mathrm{A}}}{2}\frac{1 + \frac{n_\mathrm{i}^2}{N_\mathrm{A}^2}\mathrm{e}^{(\psi_\mathrm{s}(y)-\xi(y))/V_T}}{\sqrt{\psi_\mathrm{s}(y) + V_T\frac{n_\mathrm{i}^2}{N_\mathrm{A}^2}\mathrm{e}^{(\psi_\mathrm{s}(y)-\xi(y))/V_T}}}. \tag{13}$$

Differentiating (8) and taking into account (10), the following relationship between potential variation and doping fluctuation is obtained:

$$\delta\psi_\mathrm{s} = -\frac{\alpha}{\theta + C_\mathrm{ox}}\delta N_\mathrm{A} = \tau\delta N_\mathrm{A}. \tag{14}$$

Finally, using $\delta Q_n(y) = -\delta Q_\mathrm{t}(y) - \delta Q_\mathrm{d}(y)$ and (10), (11), (14), we obtain:

$$\delta Q_n = \left[-\alpha - \theta\tau + \frac{\sqrt{2q\epsilon_\mathrm{S}}}{2}\frac{\psi_\mathrm{s} + \tau N_\mathrm{A}}{\sqrt{N_\mathrm{A}\psi_\mathrm{s}}}\right]\delta N_\mathrm{A} = \beta\delta N_\mathrm{A}. \tag{15}$$

Equations (14) and (15) provide the relevant expressions for evaluating the drain current fluctuation, which is derived as follows. First, we linearize (9):

$$\delta I_\mathrm{D} = -W\mu_n\left[\delta Q_n\frac{\mathrm{d}\psi_\mathrm{s}}{\mathrm{d}y} + Q_n\frac{\mathrm{d}\delta\psi_\mathrm{s}}{\mathrm{d}y} - V_T\frac{\mathrm{d}\delta Q_n}{\mathrm{d}y}\right], \tag{16}$$

where $\mathrm{d}\psi_\mathrm{s}/\mathrm{d}y$ is expressed as

$$\frac{\mathrm{d}\psi_\mathrm{s}}{\mathrm{d}y} = -\frac{I_\mathrm{D}}{W\mu_n}\left[Q_n + V_TC_\mathrm{ox}\left(1 + \frac{\gamma}{2\sqrt{\psi_\mathrm{s}}}\right)\right]^{-1}. \tag{17}$$

Using an input spatially impulsive dopant density fluctuation $\delta N_\mathrm{A}(y) = C\delta(y-y_0)$, and integrating both sides of (16) along the channel (or up to the pinch off point, if this is placed before the drain), we finally obtain the Green's function $G(y_0) = \delta I_\mathrm{D}/C$ relating the two variations:

$$G(y_0) = -\frac{W\mu_n}{L'}\left[\beta(y_0)\left.\frac{\mathrm{d}\psi_\mathrm{s}}{\mathrm{d}y}\right|_{y_0} - \tau(y_0)\left.\frac{\mathrm{d}Q_n}{\mathrm{d}y}\right|_{y_0}\right], \tag{18}$$

where $L' \leq L$ is the length of the channel portion where no pinch off occurs (i.e., the so-called ohmic part of the channel).

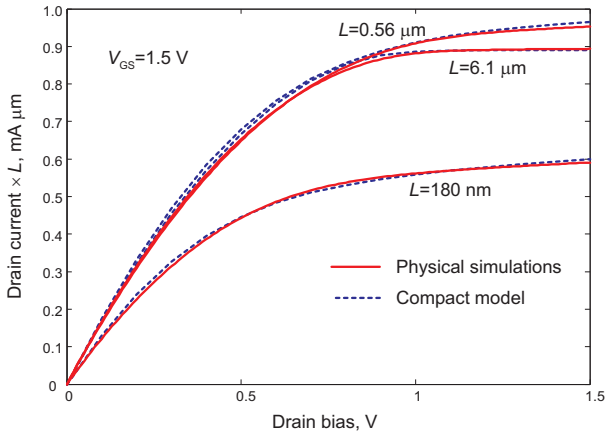

Fig. 3. DC output characteristics of the three MOSFET devices: comparison between the physical simulations and the PSP compact model.

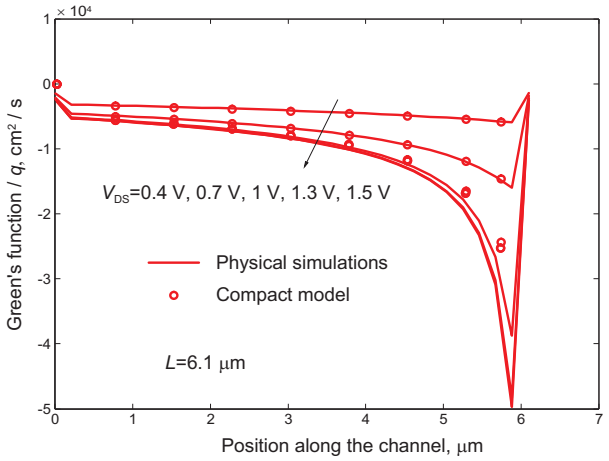

Fig. 4. Comparison between the Green's function calculated with the physical simulation and the compact model. MOSFET with $L = 6.1$ μm.

IV. Examples

In order to validate the approach, we have performed 2D drift-diffusion physics-based simulations of three nMOSFETs, characterized by a SiO_2 oxide and by the following features:

- $L = 0.56$ μm, oxide thickness $t_{ox} = 3$ nm, $N_A = 5\times10^{17}$ cm^{-3};
- $L = 6.1$ μm, $t_{ox} = 3$ nm, $N_A = 5\times10^{17}$ cm^{-3}: this long gate device has the same gate stack as the $L = 0.56$ μm MOSFET (and, therefore, the same threshold voltage) in order to compare the compact model also to a long gate device;
- $L = 180$ nm, $N_A = 1.56 \times 10^{17}$ cm^{-3}: the oxide thickness and the doping level of this device were chosen according to a constant field scaling rule with respect to the $L = 0.56$ μm MOSFET.

The simulations were performed with Synopsys Sentaurus, which implements the numerical Green's functions-based model discussed in [5].

The compact model for the Green's function discussed in Sec. III has been implemented within the framework of the PSP compact model [8] in Verilog-A exploiting the SiMKit library and the adapter devised as an interface to Agilent ADS [17]. Because of the short channel length of the simulated devices, we have also implemented in the compact model the standard short-channel effect corrections, namely channel length modulation (CLM) and drain induced barrier lowering (DIBL) [8]. The model parameters were fitted to reproduce the DC characteristics only, and were used as such also for the calculation of the Green's function.

The DC characteristics are compared in Fig. 3, showing a good agreement for all the devices considered.

Figs. 4, 5 and 6 report a comparison between the analytical Green's function we propose and the numerical value obtained through Synopsys Sentaurus TCAD simulations for the three devices. For all devices, the agreement between the numerical and analytical Green's function is good, thus demonstrating the accuracy of the proposed approach.

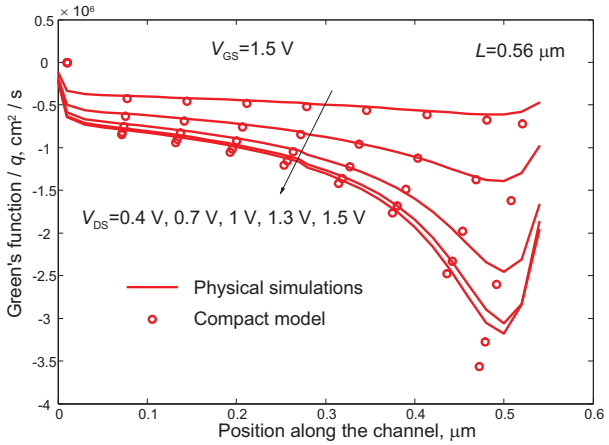

Fig. 5. Comparison between the Green's function calculated with the physical simulation and the compact model. MOSFET with $L = 0.56$ μm.

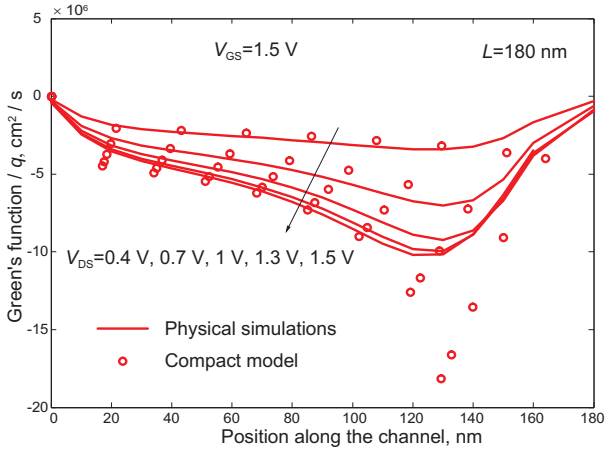

Fig. 6. Comparison between the Green's function calculated with the physical simulation and the compact model. MOSFET with $L = 180$ nm.

V. Conclusion

We have presented an analytical approach, developed within the framework of a surface-potential charge-based MOSFET compact model, to estimate the drain current variability induced by random dopant fluctuations along the channel. The approach is based on a linear perturbation theory, in which the total current fluctuation is expressed, according to a Green's function technique, as a spatial superposition integral involving the random dopant fluctuation arising from process variability and, as the kernel, the Green's function modeling the current fluctuation caused by a spatially impulsive dopant fluctuation. We have described in detail how the Green's function can be directly evaluated exploiting a surface-potential based charge-control compact model. Comparisons with results from 2D drift-diffusion simulations show that the analytical approach yields accurate results also for comparatively short-channel devices, thus suggesting that, perhaps with the help of some heuristic parametrization, the compact model can be able to provide predictive results also for deeply-scaled MOSFET technologies. Future work will concern the development of application examples including space-dependent fluctuations and the exploitation, to model the process variability, of more accurate data arising e.g. from process simulators.

Acknowledgment

This work was supported by the European Union ENIAC Joint Undertaking through the MODERN project.

References

[1] S.K. Sha, "Modeling process variability in scaled CMOS technologies", *IEEE Design and Test of Computers*, Vol. 27, No. 2, pp. 8–16, 2010.

[2] A. Asenov, A.R. Brown, J.H. Davies, S. Kaya, G. Slavcheva, "Simulation of Intrinsic Parameter Fluctuations in Decananometer and Nanometer-Scale MOSFETs", *IEEE Trans. El. Dev.*, Vol. 50, No. 9, pp. 1837–1852, Sep. 2003.

[3] Y. Li, C.-H. Hwang, T.-Y. Li, M.-H. Han, "Process-Variation Effect, Metal-Gate Work-Function Fluctuation, and Random-Dopant Fluctuation in Emerging CMOS Technologies", *IEEE Trans. El. Dev.*, Vol. 57, No. 2, pp. 437–447, Feb. 2010.

[4] A. Asenov, "Random Dopant Induced Threshold Voltage Lowering and Fluctuations in Sub-0.1 μm MOSFETs: A 3-D Atomistic Simulation Study", *IEEE Trans. El. Dev.*, Vol. 45, No. 12, pp. 2505–2513, Dec. 1998.

[5] A. Wettstein, O. Penzin, E. Lyumkis, W. Fichtner, "Random Dopant Fluctuation Modelling with the Impedance Field Method", *Proc. SISDEP 03*, pp. 91–94, 2003.

[6] C. Alexander, G. Roy, A. Asenov, "Random-Dopant-Induced Drain Current Variation in Nano-MOSFETs: A Three-Dimensional Self-Consistent Monte Carlo Simulation Study Using Ab Initio Ionized Impurity Scattering", *IEEE Trans. El. Dev.*, Vol. 55, No. 11, pp. 3251–3258, Nov. 2008.

[7] P.A. Stolk, F.P. Widdershoven, D.B.M. Klaassen, "Modeling Statistical Dopant Fluctuations in MOS Transistors", *IEEE Trans. El. Dev.*, Vol. 45, No. 9, pp. 1960–1971, Sep. 1998.

[8] X. Li, W. Wu, G. Gildenblat, G.D.J. Smit, A.J. Scholten, D.B.M. Klaassen, R. van Langevelde, *MOS model PSP*. http://www.nxp.com/models/mos_models/psp/

[9] F. Bonani, S. Donati Guerrieri, G. Ghione, "Physics-based simulation techniques for small- and large-signal device noise analysis in RF applications", *IEEE Trans. El. Dev.*, Vol. ED-50, No. 3, pp. 633–644, March 2003.

[10] F. Bonani, G. Ghione, *Noise in semiconductor devices. Modeling and simulation,* Springer Series in Advanced Microelectronics, Springer Verlag: Heidelberg, 2001.

[11] G. Ghione and F. Filicori, "A computationally efficient unified approach to the numerical analysis of the sensitivity and noise of semiconductor devices", *IEEE Trans. on CAD*, Vol. 12, p. 425, 1993.

[12] S. Donati, F. Bonani, M. Pirola, G. Ghione, "Sensitivity-based optimization and statistical analysis of microwave semiconductor devices through multidimensional physical simulation", *Int. J. Microwave and Millimeter-Wave Computer-Aided Engineering*, Vol. 7, No. 1, pp. 129–143, Jan. 1997.

[13] F. Bonani, S. Donati, F. Filicori, G. Ghione, M. Pirola, "Physics-based large-signal sensitivity analysis of microwave circuits using technological parametric sensitivity from multidimensional semiconductor device models", *IEEE Trans. Microwave Theory Techn.*, Vol. MTT-45, No. 5, pp. 846–855, May 1997.

[14] Synopsys Inc. Sentaurus Device simulator: http://www.synopsys.com/Tools/TCAD/DeviceSimulation/Pages/SentaurusDevice.aspx.

[15] Y. Tsividis, *Operation and modeling of the MOS transistor*, McGraw-Hill, New York, 1999.

[16] G. Gildenblat, X. Li, W. Wu, H. Wang, A. Jha, R. van Langevelde, G.D.J. Smit, A.J. Scholten, D.B.M. Klaassen, "PSP: An advanced surface-potential-based MOSFET model for circuit simulation", *IEEE Trans. El. Dev.*, Vol. ED-53, No. 9, pp. 1979–1993, Sept. 2006.

[17] Agilent EEsof EDA. Advanced Design System overview: http://eesof.tm.agilent.com/products/adsoview.html